13º Congresso Brasileiro de Engenharia de Fabricação
7 a 9 de maio de 2025, Salvador, BA, Brasil

COBEF2025 0035
COMPARATIVE ANALYSIS OF NUMERICAL AND EXPERIMENTAL MODELING OF YIELDING IN DUCTILE MATERIALS

Erikson Portugal[1]
Jéssica Silveira[1]
Marcos Alves Rabelo[1]
Sérgio Junichi Idehara[1]
Carlos Maurício Sacchelli[1]

[1]Federal University of Santa Catarina, Rua Dona Francisca, 8300 – Bloco U Zona Industrial Norte Joinville – SC – Brasil - CEP: 89.219-600

Abstract: *This study presents a comparative analysis of the numerical and experimental modeling of linear and plastic yielding failure in ductile materials, specifically focusing on a 1020 steel specimen subjected to a tensile test. Numerical simulations were conducted using two finite element analysis (FEA) software packages, Ansys and QForm, to evaluate their predictive capabilities regarding specimen deformation. The 1020 steel specimen was chosen due to its use in industrial applications, making it an important material for assessing the accuracy of FEA software in modeling material behavior under stress. The research involved conducting physical tensile tests on the 1020 steel specimen, measuring critical data such as stress-strain relationships, yield points, and ultimate tensile strength. These experimental results were then compared with the numerical predictions obtained from Ansys and QForm simulations. Ansys provided an analysis of stress distribution and deformation in the specimen in the linear region of the material elongation. On the other hand, QForm, which specializes in metal forming processes, offered visual results of the specimen's behavior under tensile stress, with a particular focus on the plastic deformation stages. This analysis considered a variable number of elements and nodes along the specimen length variation to map the constriction region and the level of its deformation. The comparison with the experimental data revealed similarities in the stress-strain curves, indicating a good predictive accuracy of the software package. Ansys demonstrated precision in modeling the initial elastic region, closely matching the experimental stress-strain curves. Although the results are representative of the physical behavior, some differences were noted in the prediction of the yield point, specimen elongation and ultimate tensile strength. To reduce that, this study highlights the importance of adjusting the material properties in the simulator input data. The findings underscore the need for calibration and validation of numerical models against experimental data, as for example the flow stress model constants, to ensure accurate predictions of material failure and deformation. From this study, combining different numerical approaches may improve the understanding of material behavior under complex deformation and different loading conditions.*

Keywords*: Modeling, plastic deformation, numerical model, experimental test*

1. INTRODUCTION

A tensile test is a controlled method used to characterize the mechanical properties of materials, by mapping their stress-strain behavior during elastic and plastic yielding phases. This testing process enables researchers to understand material behavior under uniaxial tension, allowing for the analysis of the onset of plastic deformation and eventual failure. The test provides parameters such as yield strength, ultimate tensile strength, and elongation, which are needed for assessing a material's capacity to withstand plastic deformation without failure (Petrík & Ároch, 2019; Kweon et al., 2021). In mechanical design and material selection, the information about the plastic yielding is necessary for predicting failure modes and ensuring the structural integrity of components under load. Plastic yielding is defined in ductile materials when the material undergoes irreversible deformation after reaching its yield point. The related studies, usually, highlight the use of numerical models to predict plastic yielding behavior. For example, Cai (2017) emphasized the application of the extended finite element method in capturing fracture initiation in steel under elevated temperatures. When the material enters the necking phase, as the stress distribution becomes non-uniform, the correlation between true stress-strain and engineering stress-strain curve is more difficult to accompany experimentally (Yao et al., 2016; Petrík & Ároch, 2019). For these cases, numerical simulations such as finite element analysis (FEA) are commonly employed to model this behavior. These models allow for an examination of material behavior under load, particularly in determining the transition from elastic to plastic deformation and the eventual onset of failure (Guo et al., 2018) or in opposite way, in understanding conformation dynamics for fabrication engineering applications. However, numerical models often require validation against experimental data, as inaccuracies in stress distribution predictions can lead to incorrect conclusions about material performance (Zhang et al., 2022; Cai, 2017).

Recent studies, such as Kweon et al. (2021), have demonstrated that combining experimental tensile data with iterative finite element methods can provide more accurate predictions of material behavior throughout both uniform and non-uniform deformation regions. Other studies have applied tensile tests in validating numerical models that simulate material deformation. For example, Børvik et al. (2003) analyzed by finite element simulations, with experimental tensile data, a prediction of the material behavior under varying strain rates and stress triaxiality. That study evaluated the fracture criteria in ductile materials. Similarly, Ho et al. (2019) demonstrated how true stress-strain curves derived from tensile tests can significantly improve the precision of finite element models for high-strength steel, particularly under large deformations. Zhang et al. (2022) further illustrated that uniaxial tensile tests, combined with FEA simulations, are highly effective in calibrating stress-strain relationships and predicting ductile fracture behavior in steel plates under different stress conditions. This approach had been used in research on constitutive models for various steel grades, including high-strength alloys (Sung et al., 2010).

In manufacturing and fabrication engineering, usually, the knowledge of material behavior during forming processes is considered for ensuring the performance in the shape and tolerance controls and reliability of structural components. In this way, an accurate model of material flow, stress-strain distributions, and failure mechanisms during processes such as extrusion or cold forging is necessary for predicting potential defects (Kang et al., 2018; Abhari, 2018). What would improve the product quality, and optimizing the production process. Abhari (2018) emphasized that numerical methods are applicable in evaluating material behavior during radial and combined extrusion. This kind of simulation of prediction of failure modes, such as folding defects, can be done before they occur in real-world applications. This predictive capability enhances dimensional accuracy, mechanical properties, and the surface finish of manufactured parts. The improvement in the determination of stress-strain curves, particularly after necking, provides the data needed to accurately model post-deformation behavior, for forming processes and the design of more durable components (Kang et al., 2018; Abhari, 2015). For example, hot forging often requires preform design to ensure uniform material flow and to prevent defects like laps or cracks. Biba et al. (2020) demonstrated the use of isothermal surfaces models to optimize preform shapes, reduce forming loads, and prevent common flow defects. Chezan et al. (2019) demonstrated how tribology and material models can reduce development times and improve the accuracy of strain and thickness predictions in the forming of automotive components. The integration of empirical tensile test data with FEM simulations allows for a more precise characterization of material behavior under both forming and operational conditions. For instance, Batalha & Button (2016) explored the hot formability of steel sheets in automotive components, using experimental tensile tests to calibrate numerical models, providing information on the formability limits and failure mechanisms during the manufacturing process.

Based on the necessity of an accurate numerical model of plastic deformation, this study aims to conduct a comparative analysis of numerical and experimental modeling of plastic yielding failure in steel. The finite element simulations were developed by using Ansys and QForm software. QForm, in particular, has been extensively used in studies to model metal forming processes, including cold and hot forging, deep drawing, and combined forming operations. For example, Gladkov et al (2015) applied QForm to predict fracture behavior in cold metal forming and deep drawing, demonstrating correlations between simulations and experimental results. Similarly, Hawryluk et al. (2021) utilized QForm to analyze thermomechanical properties during multi-stage forging processes, identifying areas prone to defects like laps and optimizing the production process.

2. MATERIALS AND METHODS

In this study, Ansys and QForm software, both based on the finite element method (FEM), were utilized to model the material behavior of 1020 steel during elongation. Numerical models were developed to replicate the experimental conditions of a tensile test, taking into account factors influencing material behavior, such as stress distribution and strain rates. The material properties, including the flow stress curve of 1020 steel, were updated from experimental data to ensure better accuracy of the simulation.

2.1. Tensile Test Set up

The experimental investigations were conducted in three phases. In the first phase, a 1020 steel sheet was acquired, and the specimens (CPs) were cut using a water jet cutting machine. The test specimens were prepared in accordance with the ABNT NBR ISO 6892-1 (2024) standard, with flat specimens selected, as shown in Fig. 1a.

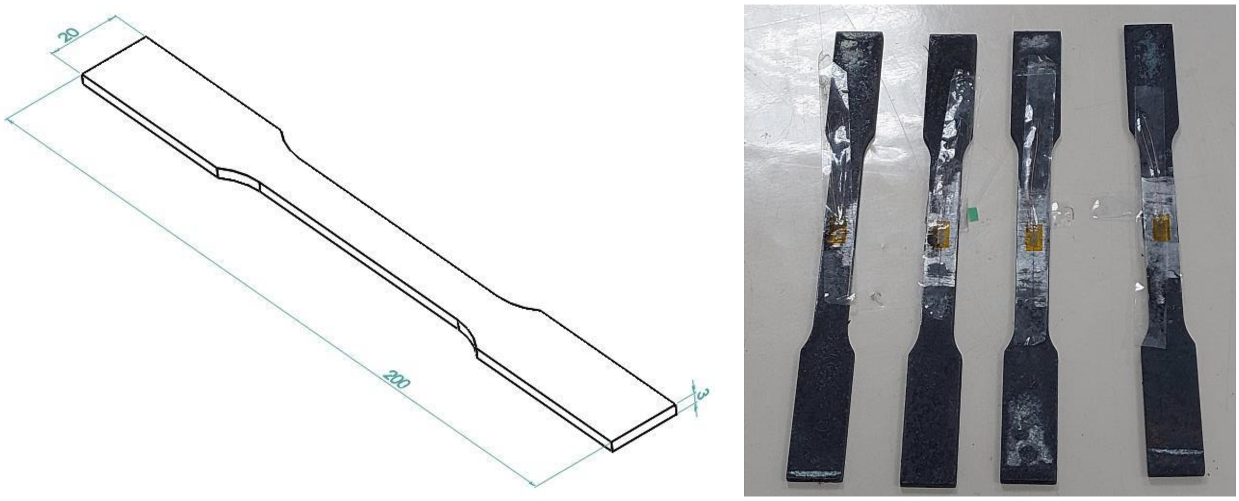

(a) (b)

Figure 1. *Illustration of the specimen based on the ABNT tensile test standard (a) and fabricated specimens with installed strain gauges (b). Dimensions are given in millimeters.*

With the specimens prepared (Fig. 1b), the second phase involved instrumenting the specimens (CPs) with uniaxial strain gauges. The mounting position for the strain gauge was determined, and a sensor and terminal were glued to each CP. Subsequently, the strain gauge wires were soldered to the terminal, followed by the welding of the sleeve cable wires. The sleeve cable serves to connect the sensors to the data acquisition system. The acquisition system channels receiving the strain gauge wires were then calibrated and prepared for measurements. The third and final phase involved setting up the universal tensile testing machine (INSTRON - 100kN). This included inputting the test parameters for the CP and mounting the specimen in the machine. To achieve precise strain measurements up to 2%, a clip gauge was used, as shown in Fig. 2a. Both a strain gauge and a clip gauge were used simultaneously to ensure a comprehensive strain measurement during the tensile test. While the clip gauge provides high-precision strain data, the strain gauge captures additional strain information directly from the specimen surface, allowing a broader evaluation of strain distribution. This redundancy improves the reliability of experimental data when compared to numerical models, ensuring a more accurate validation process. The testing procedure began with activating the data acquisition system, followed by starting the tensile test until failure (Fig. 2b). The test resulted in a stress-strain graph, providing key parameters such as the yield point, ultimate tensile strength, and fracture point.

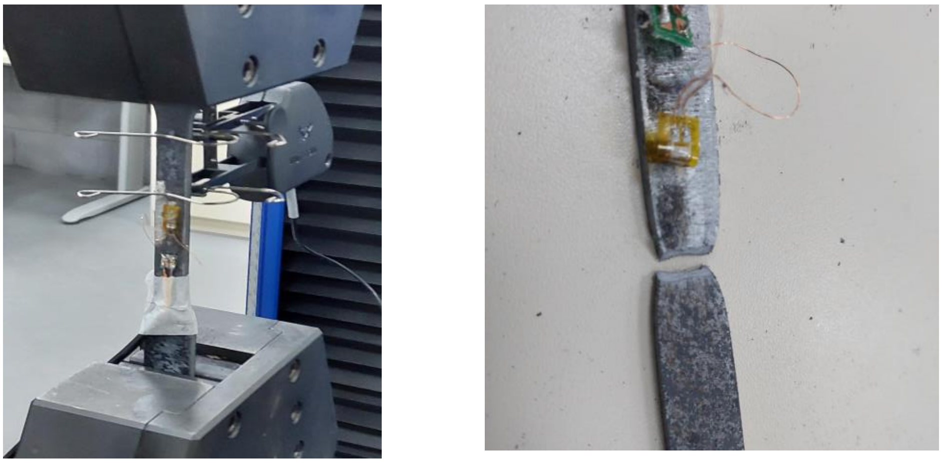

(a) (b)

Figure 2. *Specimen in the tensile testing machine (a) and the tested specimen after rupture (b).*

With the available experimental data, a comparison was performed between the numerical models developed in QForm and Ansys software.

2.2. Numerical Model from QForm

The 2D plane strain model in the QForm software is shown in Fig. 3a. In this model, Tool 1 is a movable component that pulls the specimen in the +z direction, while Tool 2 remains stationary. As a boundary condition, the velocity of Tool

1 is set to 0.0833mm/s, matching the actuator velocity of the tensile testing machine. The material used in the simulation has the properties of 1020 steel, with a density of 7,870kg/m³, an elastic modulus of 204,430.00MPa (from experimental average data), a Poisson's ratio of 0.29 (adjusted during the simulation), and a yield stress of 293.0MPa (from experimental average data).

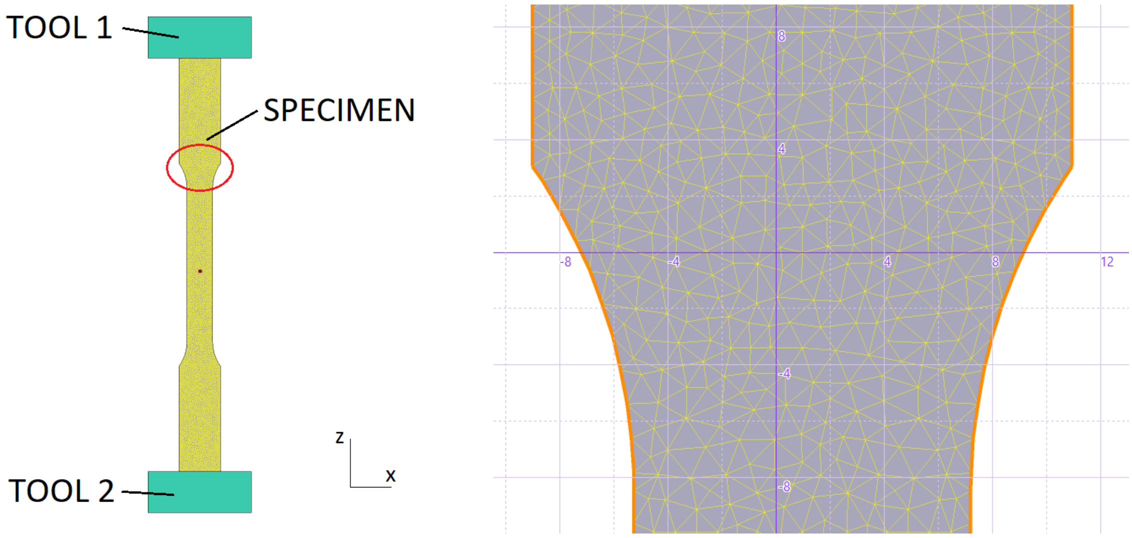

(a) (b)

Figure 3. *Model of the specimen in QForm software for the tensile test (a), and an enlarged view showing finite elements and nodes in the highlighted area (b).*

The program discretizes the specimen into triangular elements, which are dynamically remeshed throughout the simulation. The initial finite element discretization consists of 4,405 nodes and 8,309 elements, as shown in Fig. 3b. The simulation provides stress and strain data during the specimen's deformation, as well as the evolving shape of its central constriction.

From the experimental curve of Sample 1, a nonlinear regression technique was employed to determine the parameters of the Hansel and Spittel (HS) equation. These parameters were then applied in the QForm software to accurately describe the material's behavior throughout the elastic-plastic deformation phase. The flow stress model (σ) is expressed in function of deformation (ϵ) and deformation rate ($\dot{\epsilon}$) as:

$$\sigma = A_1 . exp(-m_1 . T) . \epsilon^{m_2} . exp(-m_4 . \epsilon) . \dot{\epsilon}^{m_3} \tag{1}$$

The Hansel-Spittel model was selected for this study due to its flexibility in representing flow stress behavior in a wide range of deformation conditions, including strain hardening effects. Although it is commonly applied in high-temperature forming processes, it is also suitable for cold deformation scenarios when calibrated correctly. This is particularly useful when modeling complex material behaviors where strain rate and plastic flow characteristics need to be finely tuned, as in this study. The Ludwig-Hollomon model, while widely used for describing strain hardening at room temperature, assumes a simplified power-law relationship between stress and strain, which may not fully capture nonlinear hardening effects observed in the experimental tensile test data. Given that QForm allows the integration of strain rate dependency and material flow behavior in its solver, the Hansel-Spittel model was chosen to better fit the experimental data and ensure accuracy in predicting plastic deformation.

The adjusted parameters for the Hansel and Spittel model are as follows: $A_1 = 293.0MPa$, corresponding to the yield stress, while the model constants are $m_1 = 0$ (indicating no temperature variation in this case), $m_2 = 0.2578$, $m_3 = -0.1593$ and $m_4 = 1.9242$. The update process, illustrated in Fig. 4, shows that the adjusted model provides higher precision at lower strain values but exhibits greater deviation between the experimental and simulated curves at higher strain levels.

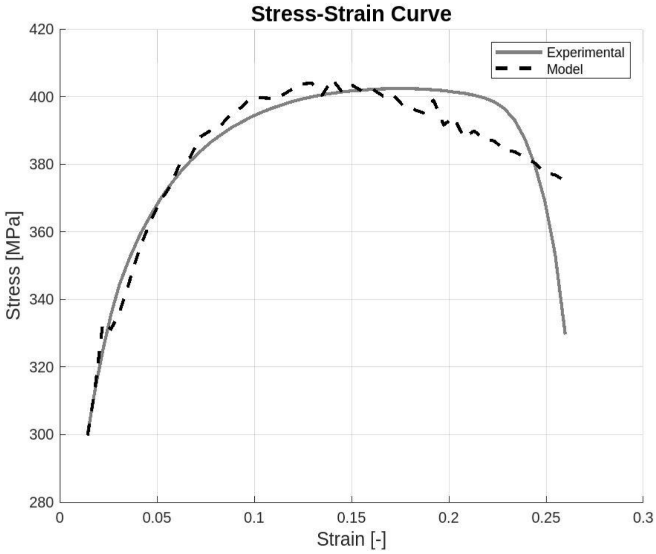

Figure 4. *Illustration of the stress-strain curve from the flow stress model adjusted using experimental tensile test data (Sample 1).*

2.3. Numerical Model from Ansys

A similar analysis was conducted using Ansys software. The CAD model employed was the same as that used in the previous QForm model, representing the test specimen geometry shown in Fig. 1a. The numerical model in Ansys, illustrated in Fig. 5, is based on a bilinear isotropic hardening model, which is capable of representing the linear region of the material's elongation curve. The simulation properties were identical to the material characteristics used in the QForm model, as described in Section 2.2. The mesh comprised 12,180 elements and 63,360 nodes, with element sizes of 1 mm. The boundary conditions included a fixed constraint on the bottom side of the specimen and a constant force applied to the opposite side (the upper face of the specimen). Simulations were performed with varying force amplitudes to generate stress-strain plots for the linear regime of the tensile test.

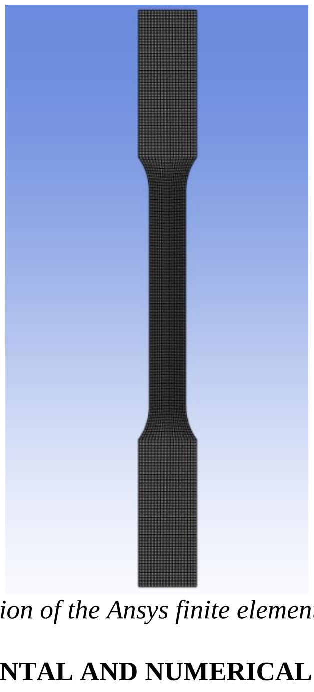

Figure 5. *Illustration of the Ansys finite element model of the specimen.*

3. COMPARISON BETWEEN EXPERIMENTAL AND NUMERICAL RESULTS

The modeling process for the finite element model requires accurate material property data, as discussed in Section 2. To input these material properties, data from experimental tensile tests were analyzed to determine the elastic modulus and the average yield strength. Fig. 6 illustrates the linear region of the stress-strain curve during specimen elongation. For comparison, the continuous black line represents the measurement from the strain gauge installed on the specimen body, the gray dashed line represents data from the machine displacement sensor (clip gauge), and the gray dot-dash curve corresponds to the Ansys model. The Ansys model shows good agreement with the stress-strain relationship measured by the tensile test machine sensor. The von Mises stress distribution in the specimen, as simulated by Ansys, is shown in Fig. 7. This stress mapping is based on an elastic model and has limitations in accurately predicting the location and behavior of material failure (plastic deformation).

Using the linear portion of the data, regression analysis determined an average elastic modulus of 204,430 MPa, with a standard deviation of 4,483.7 MPa. The mean yield stress was calculated as 292.0 MPa, with a standard deviation of 10.8 MPa.

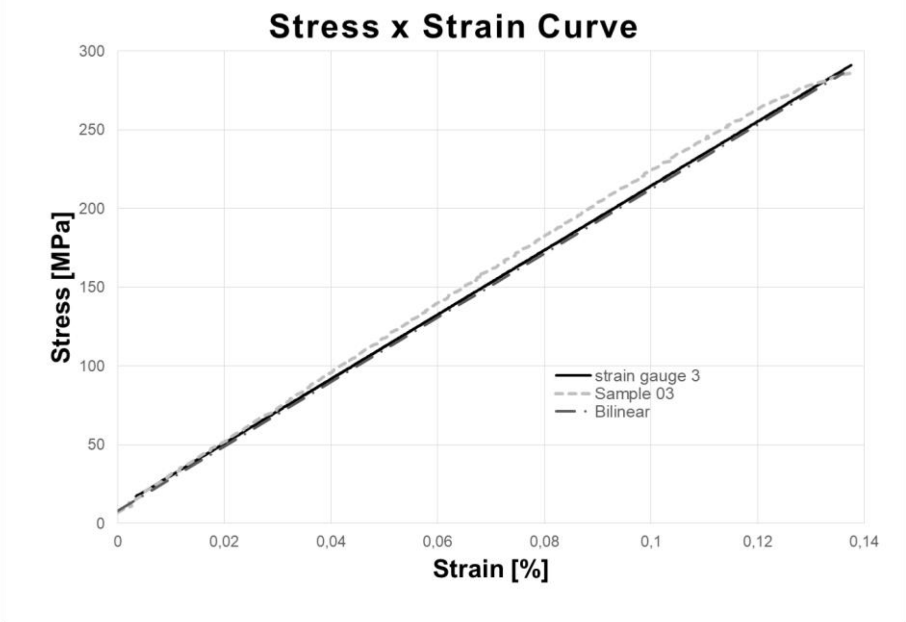

Figure 6. *Curve from the external strain gauge and machine measurements.*

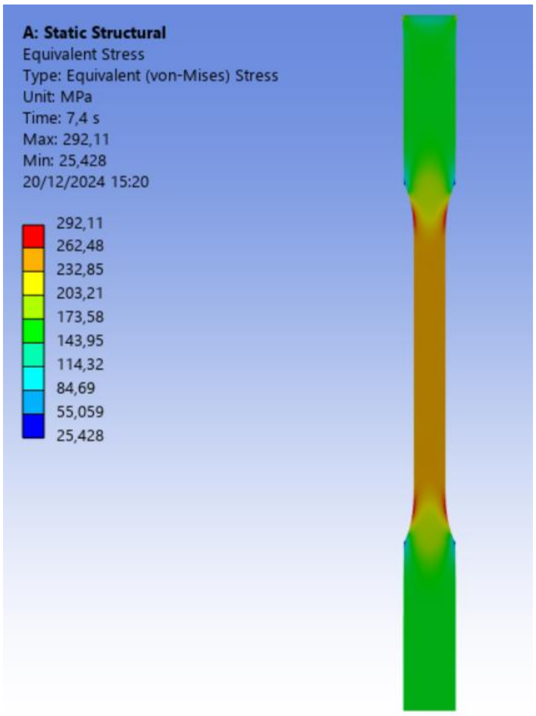

Figure 7. *Von Mises stress distribution along the specimen in the Ansys model.*

In the experimental tests, stress-strain data were collected from five samples, as shown in Fig. 8. These stress-strain curves demonstrated consistent and closely aligned results across the samples, providing a reliable experimental reference for the material's actual behavior. This data was subsequently used to simulate the numerical model for the material's plastic deformation process.

The finite element analysis in QForm produced a curve, as shown in Fig. 8, which compares the numerical model's results with the experimental data. The average maximum stress of the experimental samples was 413.17 MPa, while the numerical model predicted a maximum stress of 375.45MPa in the failed region. This 9.13% difference demonstrates a good correlation between the experimental behavior and the simulated model generated by QForm software. Additionally, the specimen deformation and stress reduction during the test are of the same order of magnitude in both the experimental results and the simulation, approximately 0.28 mm/mm. However, the model did not accurately represent the moment of structural rupture, likely due to the imprecise region in the updated model, as shown in Fig. 4. According to Tab. 1, the overall length variation of the specimen after rupture in the tensile test was approximately 9.8% relative to the initial specimen length of 200 mm, resulting in a mean length change of 19.7 mm. Similarly, the QForm model predicted a total length variation of 10.8 mm (5.4%), a difference from the initial length of 4.45% compared to the experimental results. Therefore, the numerical simulation achieved a similar representation of the material's behavior in the plastic deformation phase.

The results obtained in this study align with previous research on numerical-experimental validation of tensile tests. Børvik et al. (2003) and Zhang et al. (2022) demonstrated the effectiveness of finite element models in predicting stress-strain behavior, though variations in yield stress predictions were observed, similar to the differences noted in this study. Additionally, Ho et al. (2019) emphasized the importance of using true stress-strain curves from experimental tests to refine FEM simulations, supporting the approach taken in this research to calibrate the Hansel-Spittel model. These comparisons reinforce the necessity of integrating experimental data into numerical models to enhance their predictive accuracy, particularly for plastic deformation analysis.

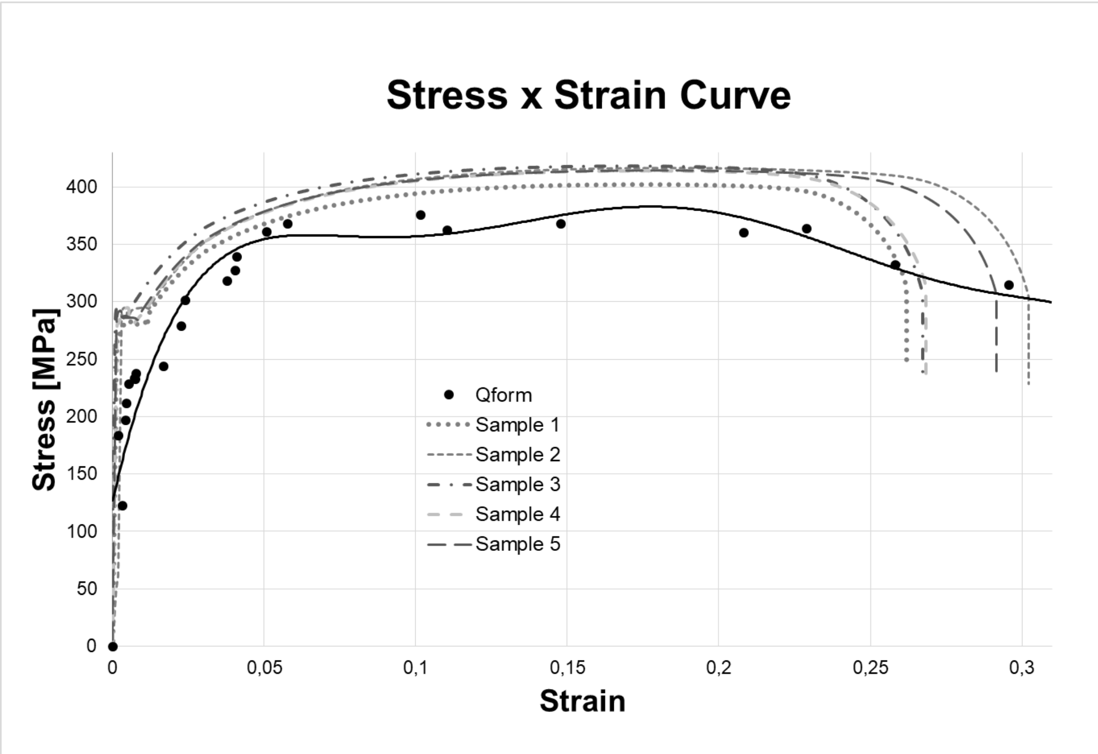

Figure 8. *Comparative stress-strain curves from the experimental tensile test and numerical models.*

Table 1. *Final length of the CP after rupture. Initial length: 200 mm.*

Sample/ Simulation	Final Length [mm]	Variation [%]
Sample 1	218.9	9.45
Sample 2	221.1	10.55
Sample 3	219.9	9.95
Sample 4	217.9	8.95
Sample 5	220.5	10.25
QForm Model	210.8	5.4

To illustrate the behavior of the test specimen during the numerical simulation, Fig. 9 provides a side-by-side comparison of the experimental test and the QForm analysis. In both cases, the fracture occurred away from the center of the specimen, at the point where stress was highest. This behavior was consistently observed in both the finite element model (QForm) and the experimental test. However, the orientation of the 45° shear plane differed between the two (Fig. 9 in zoom). This discrepancy arises because the numerical model employed a 2D plane element for the analysis. The experimental specimen exhibited a failure plane in the transverse direction (perpendicular to the body plane), while the numerical model predicted a failure plane in the lateral direction. These results underscore the potential of numerical methods to accurately predict fracture locations and regions of significant deformation and stress. However, the choice of model type and numerical elements can influence the interpretation of physical reality. This consideration is particularly important when evaluating plastic deformation and optimizing tool design in fabrication processes.

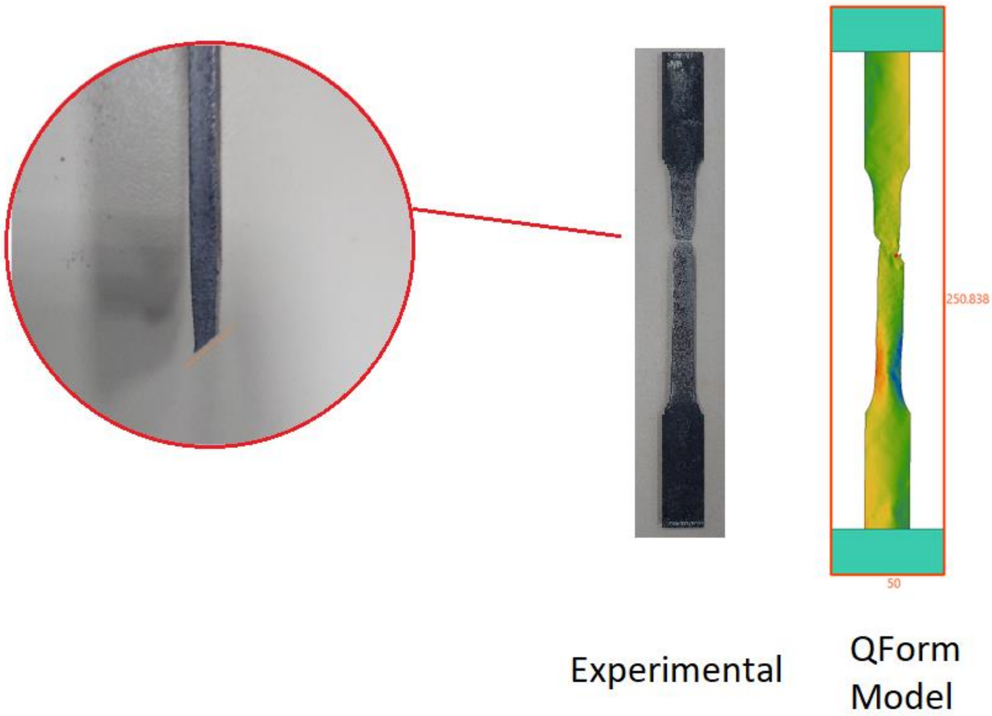

Figure 9. *Illustration of the rupture location in the specimen. Left: photographs of the real sample after the test. Right: QForm simulation.*

4. CONCLUSION

This study presented a comparative analysis of experimental and numerical modeling approaches for predicting linear and plastic yielding behavior in 1020 steel under tensile test conditions. By combining experimental tensile tests with finite element simulations using Ansys and QForm software, the study assessed the strengths and limitations of these tools in accurately modeling material behavior under stress and deformation. QForm effectively simulated the plastic flow and strain hardening phases, providing a visual interpretation of the material's deformation during the yield phase. When the numerical model was calibrated using the experimental curve, only a small difference was observed in the predictions of the yield point and ultimate tensile strength. The Hansel and Spittel model was updated using a nonlinear system solver to determine the four constants for the stress-strain relationship. As a result, the QForm model achieved a percentage difference of less than 4.0% in maximum stress and less than 5.0% in the final specimen length compared to the initial specimen length. In Ansys, the simulation of the linear part of the elongation showed strong correlation with the experimental stress-strain relationship, highlighting the software's ability to accurately represent linear deformation and stress in bodies subjected to forces. The results indicate that numerical simulations based on finite element methods (FEM) are representative of physical phenomena and can be used to understand and predict material behavior for engineering applications, particularly in the design of fabrication processes. Integrating numerical methods with experimental data enhances the accuracy of material models, especially for complex deformation scenarios encountered in industrial forming and manufacturing processes. In conclusion, the study emphasizes the importance of a systematic approach to selecting and validating numerical tools for specific material modeling tasks. Future research should focus on integrating advanced material models and considering dynamic factors, such as temperature effects, to further refine the predictive capabilities of FEM-based simulations in engineering applications.

5. ACKNOWLEDGMENTS

The authors thank SixPro for their assistance with the QForm simulations and the Fundação de Desenvolvimento da Pesquisa – Fundep Rota 2030/Linha IV 27194*37 for financial support.

6. REFERENCES

Abhari, P. The study of folding defects during the radial-forward extrusion in the enclosed dies. International Journal of Science and Research, 6, 7, pp.1746–1749, 2015.

Abhari, P. Computer-aided simulation to investigate material flow in combined-radial extrusion. International Journal of Engineering Research and Advanced Technology, 4, 2, pp.24–28, 2018.

ABNT NBR ISO 6892-1. Metallic materials - Tensile testing. Part 1: Method of test at room temperature. Associação Brasileira de Normas Técnicas, 2024.

Batalha, M.H.F.; Button, S.T. Hot formability of DIN 27MnCrB5 steel sheets under controlled thinning. Journal of Materials Processing Technology, 228, pp.98–105, 2016.

Biba, N.; Vlasov, A.; Krivenko, D.; Duzhev, A.; Stebunov, S. Closed die forging preform shape design using isothermal surfaces method. Procedia Manufacturing, 47, pp.268–273, 2020.

Borvik, T.; Hopperstad, O.S.; Berstad, T. On the influence of stress triaxiality and strain rate on the behaviour of a structural steel. Part II. Numerical study. European Journal of Mechanics A/Solids, 22, pp.15–32, 2003.

Cai, W. Fracture simulation of structural steel at elevated temperature using XFEM technique. IOP Conf. Series: Materials Science and Engineering, 264, pp.1–10, 2017.

Chezan, A.R.; Khandeparkar, T.V.; ten Horn, C.H.L.J.; Sigvant, M. Accurate sheet metal forming modeling for cost effective automotive part production. IOP Conf. Series: Materials Science and Engineering 651, pp.1–8, 2019.

Gladkov, Y.; Peshekhodov, I.; Vucetic, M.; Bouguecha, A.; Behrens, B.-A. Implementation of the Bai & Wierzbicki fracture criterion in QForm and its application for cold metal forming and deep drawing technology. MATEC Web of Conferences 21, pp.1–7, 2015.

Guo, H.; Xiao, F.; Liu, Y.; Liang, G. Experimental and numerical study on the mechanical behavior of Q460D high-strength steel bolted connections. Journal of Constructional Steel Research 151, pp.108–121, 2018.

Hawryluk, M.; Rychlik, M.; Ziemba, J.; Jasiak, K.; Lewandowski, F.; Dudkiewicz, L. Analysis of the production process of the forked forging used in the excavator drive system in order to improve the currently implemented technology by the use of numerical modeling. Materials Science-Poland, 39, 2, pp.227–239, 2021.

Ho, H.C.; Chung, K.F.; Liu, X.; Xiao, M.; Nethercot, D.A. Modelling tensile tests on high strength S690 steel materials undergoing large deformations. Engineering Structures, 192, pp.305–322, 2019.

Kang, L.; Ge, H.; Suzuki, M.; Wu, B. An average weight whole-process method for predicting mechanical and ductile fracture performances of HSS Q690 after a fire. Construction and Building Materials 191, pp.1023–1041, 2018.

Kweon, H.D.; Kim, J.W.; Song, O.; Oh, D. Determination of true stress-strain curve of type 304 and 316 stainless steels using a typical tensile test and finite element analysis. Nuclear Engineering and Technology, 53, pp.647–656, 2021.

Petrík, A.; Ároch, R. Usage of true stress-strain curve for FE simulation and the influencing parameters. IOP Conf. Series: Materials Science and Engineering, 566, pp.1–7 2019.

Petrov, P.; Matveev, A.; Kulikov, M.; Stepanov, B.; Petrov, M.; Burlakov, I.; Dixit, U.S. Finite-element modelling of forging with torsion: investigation of heat effect. Procedia Manufacturing, 47, pp.274–281, 2020.

Sung, J.H.; Kim, J.H.; Wagoner, R.H. A plastic constitutive equation incorporating strain, strain-rate, and temperature. International Journal of Plasticity, 26, pp.1746–1771, 2010.

Yao, D.; Cai, L.; Bao, C. A new fracture criterion for ductile materials based on a finite element aided testing method. Materials Science & Engineering A, 673, pp.633–647, 2016.

Zhang, Y.; Liu, Y.; Yang, F. Ductile fracture modelling of steel plates under tensile and shear dominated states. Journal of Constructional Steel Research, 197, pp.1–14, 2022.

RESPONSIBILITY NOTICE